

We are IntechOpen, the world's leading publisher of Open Access books Built by scientists, for scientists

6,900

Open access books available

185,000

International authors and editors

200M

Downloads

Our authors are among the

154

Countries delivered to

TOP 1%

most cited scientists

12.2%

Contributors from top 500 universities



WEB OF SCIENCE™

Selection of our books indexed in the Book Citation Index
in Web of Science™ Core Collection (BKCI)

Interested in publishing with us?
Contact book.department@intechopen.com

Numbers displayed above are based on latest data collected.
For more information visit www.intechopen.com



Sintering Behavior of Vitrified Ceramic Tiles Incorporated with Petroleum Waste

A.J. Souza, B.C.A. Pinheiro and J.N.F. Holanda

Additional information is available at the end of the chapter

<http://dx.doi.org/10.5772/53256>

1. Introduction

Currently, the urgent need to preserve the environment has aroused great interest in academic and industrial areas for the reuse of pollutant wastes. In the XXI century one of the challenges of the environmental sustainability of the planet is to seek solution to the final disposal of huge volumes of pollutant wastes produced every year.

The petroleum industry generates various types of oily sludges in its production chain [1]: i) extraction of crude oil from the ground; ii) transportation to refineries and product distribution centers; iii) refining into finished products; and iv) marketing or sale of the products to consumers. These oily sludges are basically composed by hydrocarbons in the form of oil, water, solids, and traces of heavy metals in different proportions according to each area. For this reason, the oily sludges are considered as being hazardous waste materials. Thus, the petroleum industry is confronted with the environmental problem of the correct management of huge amounts of oily sludges produced worldwide.

Recently, the Brazilian petroleum industry has presented high growth in the production of crude oil. As a result, Brazilian oil industry generates huge volume of oily sludge during the oil extraction process. The traditional disposal methods used for management of this oily sludge include storage in ponds, dikes, and biodegradation (landfarming) [2,3]. More recently, the oily sludge has been treated with bentonite clay for disposal in sanitary sites, resulting in a new waste material that hereafter will be named as petroleum waste [4]. However, these waste management options are very limited, costing money and environmental impact.

Nowadays, the reuse of waste materials as an alternative raw material in the production of ceramic materials for civil construction has become a very attractive method [5-7]. The reuse approach is environmentally correct and can contribute to the environmental sustainability,

resulting in three main advantages: i) use of low cost raw material; ii) the conservation of the natural resources; and iii) the management of a pollutant waste.

The reuse of petroleum waste into ceramic materials for civil construction has already been investigated [2-4,8-11]. However, the sintering behavior of floor tiles containing petroleum waste during the firing step, which is a complex process, is not still thoroughly understood. Floor tiles are a multicomponent system primarily composed of clays, feldspar, and quartz, and is considered to be one of the most complex ceramic materials [12].

This chapter focuses on the sintering behavior of vitrified floor tiles containing petroleum waste. Emphasis is given on the effects of the petroleum waste additions on the sintering behavior, microstructural evolution, and physical properties of the vitrified floor tiles.

2. Experimental details

The raw materials used are commercial kaolin, Na-feldspar, quartz, and petroleum waste from petroleum extraction industry from south-eastern Brazil. The petroleum waste sample is a solid material in the form of granular powder. The raw materials were dried at 110 °C, dry-ground, and then passed through a 325-mesh (45 µm ASTM) sieve. The chemical and mineralogical compositions are given in Table 1. The processing flow diagram is shown in Fig. 1.

Oxides	kaolin	Petroleum Waste	Na-feldspar	Quartz
SiO ₂	49.07	41.73	69.55	09.97
Al ₂ O ₃	33.74	10.93	18.82	0.41
Fe ₂ O ₃	0.22	7.63	0.14	0.01
TiO ₂	0.01	0.52	0.02	0.02
Na ₂ O	0.52	0.44	9.63	0.13
K ₂ O	1.97	0.95	1.47	0.18
CaO	0.30	7.76	0.17	0.01
MgO	0.06	5.87	0.09	0.01
MnO		0.02		
P ₂ O ₅		0.09		
BaO		5.03		
SrO		0.29		
Loss on ignition	14.01	18.74	0.32	0.26
Mineral phases	kaolinite, quartz	quartz, kaolinite, barite, calcite, gypsum, hematite, galena, halite, calcium chloride, potassium chloride, montmorillonite	albite, quartz	quartz

Table 1. Chemical (wt.%) and mineralogical compositions of the raw materials.

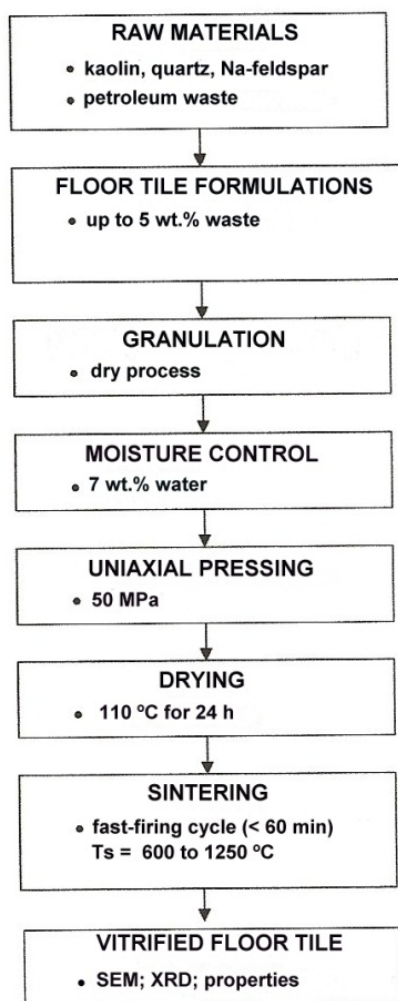


Figure 1. Process flow diagram of the vitrified floor tiles.

Several floor tile compositions were prepared using mixtures of kaolin, Na-feldspar, quartz, and petroleum waste (Table 2). The petroleum waste additions were up to 5 wt.% in gradual replacement of kaolin. The floor tile formulation used as a reference consisted of 40 wt.% kaolin, 47.5 wt.% Na-feldspar, and 12.5 wt.% quartz.

Raw materials	Tile formulations (wt.%)		
	MT1	MT2	MT3
Kaolin	40	37.5	35
Waste	0	2.5	5
Na-feldspar	47.5	46.5	47.5
Quartz	12.5	12.5	12.5

Table 2. Composition of the floor tile formulations containing petroleum waste.

The floor tile formulations (Table 2) were mixed, homogenized, and granulated via dry process using a high intensity mixer. After granulation step, the granules coarser than 2 mm were discarded. The moisture content (moisture mass/dry mass) was adjusted to 7 %.

Mineralogical analysis of the floor tile formulations was done using Cu-Ka radiation and 1.5° (2θ)/min scanning speed in a conventional diffractometer. Mineral phases were identified by comparing the intensities and positions of the Bragg peaks to those listed in the JCPDS/ICDD data files.

Thermogravimetric analysis (TGA and DrTGA) of the floor tile powder sample was performed in air between 25 °C and 1200 °C using a heating rate of 10 °C/min. Dilatometric analysis of the floor tile samples was carried out on unfired test pieces within the 25 – 1200 °C temperature range using a heating rate of 10 °C/min under air atmosphere.

The tile powders were uniaxially pressed into test bars (11.5×2.54 cm²) under a load of 50 MPa, and then dried at 110°C. The sintering step was carried out at soaking temperatures varying from 600 to 1250 °C, using a fast firing-cooling cycle of total duration < 60 min. The heating and cooling rates used in this work were chosen to simulate actual sintering process used in the tile industry.

The following physical properties of the floor tile pieces have been determined: linear shrinkage, water absorption, apparent density, and apparent porosity.

The linear shrinkage values were obtained by measuring the length of the rectangular specimens before and after sintering step using a caliper with a precision of ± 0.01 .

Water absorption values were determined from weight differences between the as-sintered and water saturated samples (immersed in boiling water for 2h) according to the ASTM C373 standardized procedures [13].

The apparent density of the floor tile pieces were determined by the Archimedes method according to the ASTM C373 standardized procedures [13].

The apparent porosity also was determined according to the ASTM C373 standardized procedures [13].

Scanning electron microscopy operating at 15 kV was used to examine the gold-coated fracture surfaces of the sintered floor tile pieces via secondary electron images (SEI/SEM).

The crystalline phases after sintering were identified between $2\theta = 10^\circ$ and $2\theta = 80^\circ$ via X-ray diffraction analysis with Cu-Ka radiation (40 kV, 40 mA). The mineral phases were identified using reference data from the JCPDS/ICDD data files.

3. Results and discussion

3.1. Characteristics of the floor tile formulations

The XRD pattern of the MT1 sample is shown in Fig. 2. The reference formulation exhibits peaks that are characteristics of kaolinite ($\text{Al}_2\text{O}_3 \cdot 2\text{SiO}_2 \cdot 2\text{H}_2\text{O}$), albite ($\text{NaAlSi}_3\text{O}_8$), and quartz

(SiO_2). XRD pattern of the petroleum waste containing formulation (MT3 sample) is shown in Fig. 3. In addition to kaolinite, albite, and quartz, peaks of barite (BaSO_4), hematite (Fe_2O_3), calcium sulphate (CaSO_4), and montmorillonite were identified. These results are in accordance with the raw materials data (Table 1).

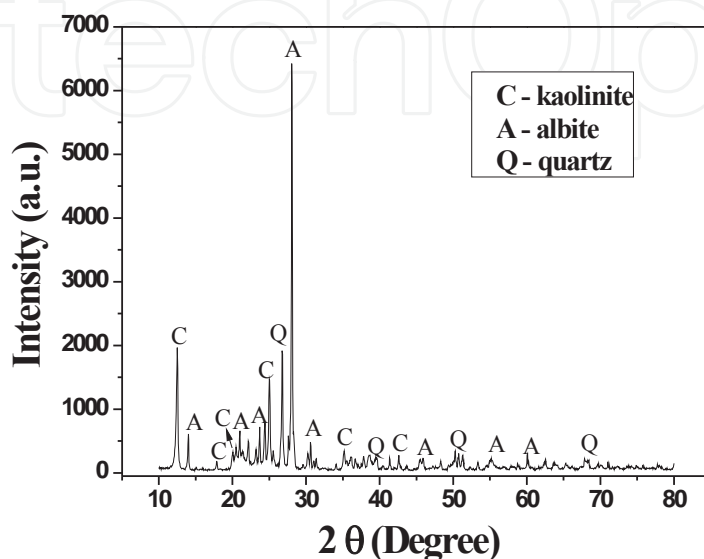


Figure 2. XRD pattern of the MT1 sample (waste-free formulation).

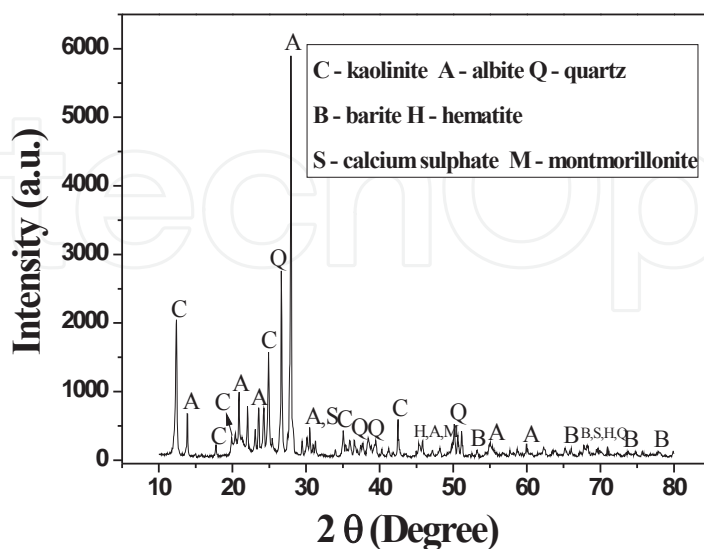


Figure 3. XRD pattern of the MT3 sample (with 5 wt.% petroleum waste).

The thermogravimetric curves (TGA and DrTGA) for the MT2 sample (with 2.5 wt.% petroleum waste) is shown in Fig. 4. DrTGA curve shows that the floor tile formulation exhibit one endothermic event around 573.5 °C. This endothermic event is related mainly to the dehydroxylation of kaolinite. In addition, this endothermic reaction corresponds to an intense process of mass transfer in the tile sample as observed in the TG curve. The MT2 sample presented a total weight loss during sintering around 4.4 %. In addition the removal of chemically bound water of the kaolinite structure, the volatilization of oil (hydrocarbons) of the petroleum waste should be also considered.

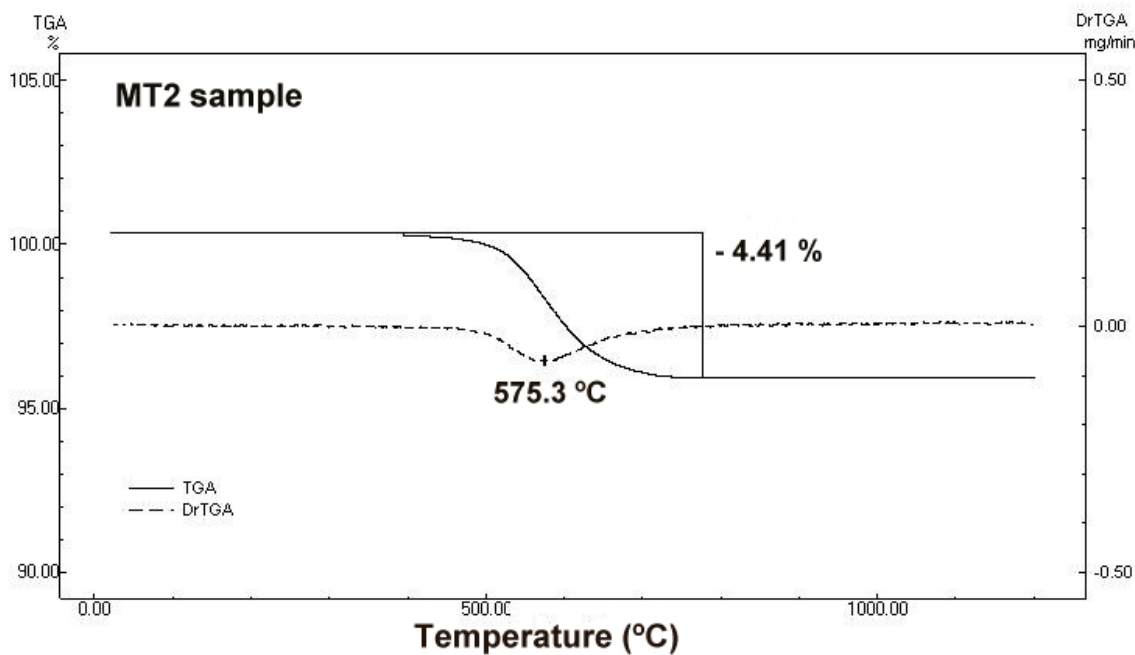


Figure 4. TGA/DrTGA curves of the MT2 sample.

Table 3 gives the particle size distribution of the raw materials used. The results revealed that the raw materials presented high concentration (83.2 – 96.8 %) of mineral particles < 63 µm. This means that the raw materials used in the floor tile formulations have good degree of comminution that could favor the reactivity of the particles during the sintering process. It also prevents the segregation of non-plastic and plastic components present in the tile formulations.

Particle size	Kaolin	Petroleum Waste	Albite	Quartz
< 2 µm	22.9	12	5	9.6
2 < x < 63 µm	73.9	83	89	73.6
63 < x < 200 µm	3.2	5	6	16.8

Table 3. Particle size distribution of the raw materials (wt.%).

3.2. Phase evolution during sintering

The XRD patterns of the MT1 samples sintered between 600 and 1250 °C are presented in Fig. 5. Based on the X-ray diffraction patterns and previous studies [14-17] it is possible to describe the phase transformations underwent by the waste-free floor tile formulation (MT1 sample) at different temperatures.

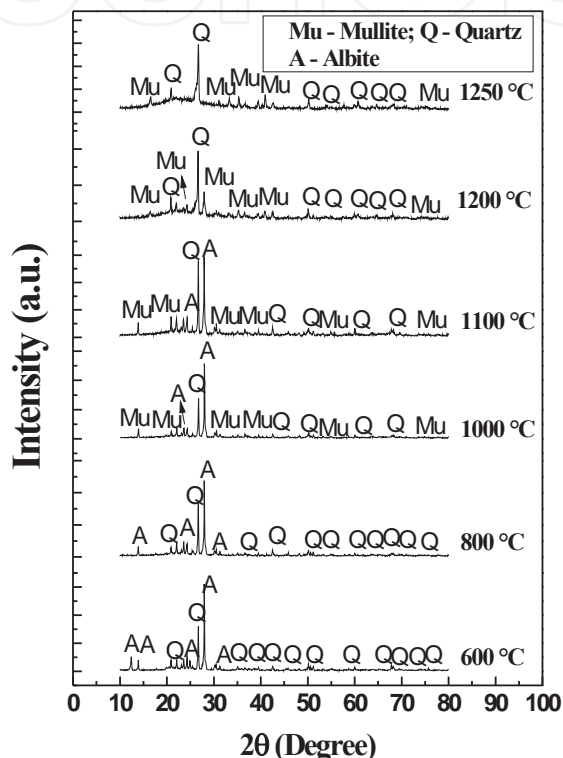
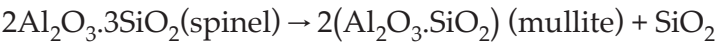
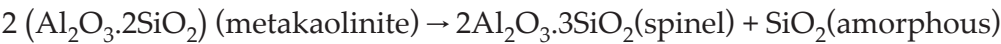


Figure 5. XRD patterns of the MT1 sample sintered at different temperatures.

The phase transformations involved in the waste-free floor tile body (MT1 sample) during sintering could be described as follow. The evolution of the physically adsorbed water by the mineral particles takes place until 100 °C ($\text{H}_2\text{O}_{(l)} \rightarrow \text{H}_2\text{O}_{(g)}$). At 573 °C, α - β quartz inversion of free silica occurs. At 600 °C, the characteristic peaks of kaolinite have disappeared. In fact, between ~ 450 and 600 °C, kaolinite loses the OH groups of the gibbsite sheet leading to the formation of amorphous metakaolinite according to:



At 800 °C, the peaks of quartz and albite are still seen. At 1000 °C, peaks of mullite appear. In this temperature range, the silicate lattice totally collapse, followed by reorganization of the metakaolinite structure and the formation of amorphous silica. A spinel structure is formed and then quickly transformed to mullite according to:



It can be seen that the mullite peaks increasing in intensity with the sintering temperature, but the quartz peaks decreasing slightly due its partial dissolution. Above 1100 °C the albite peaks are not seen. At 1200 °C, an amorphous band between $2\theta = 15^\circ$ and $2\theta = 25^\circ$ can be also observed. This is due to the fusion of albite to form a viscous liquid phase, which is then cooled to glass.

The XRD patterns of the MT3 formulation (with 5 wt.% petroleum waste) sintered between 600 and 1250 °C are shown in Fig. 6. In addition the mullite and quartz, characteristic peaks of barite, hematite, and calcium sulphate were also identified. These results are in agreement with the chemical composition data (Table 1) and X-ray diffraction (Fig. 2). Thus, the partial replacement of kaolin with petroleum waste influenced the phase evolution of the vitrified floor tiles. This means that the petroleum waste addition can influence the sinterability of the floor tile formulations.

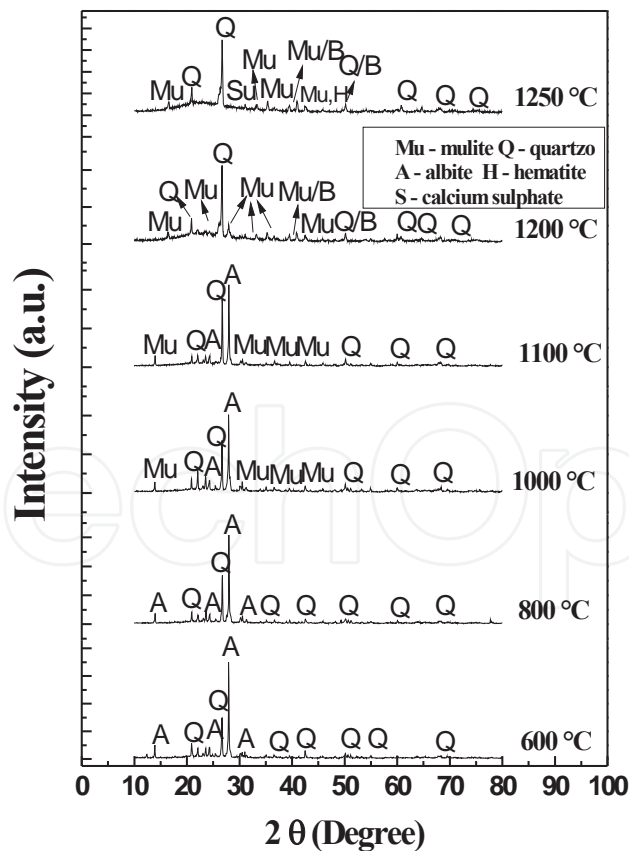


Figure 6. XRD patterns of the MT3 sample sintered at different temperatures.

3.3. Microstructural analysis of the sintered floor tiles

The microstructure of fractured surface of MT1 sample (waste-free sample) sintered at 1210 °C obtained via SEI/SEM is shown in Fig. 7. One can clearly observe that the microstructure is composed mainly of dense zones (glassy phase) connected with rugous zones (open porosity). As indicated by the XRD analysis (Fig. 5), it consists of mullite, quartz, and glassy phase. In addition, the open pore volume is essentially formed by a narrow channels structure of irregular morphology. This means that the densification of the MT1 sample during sintering at 1210 °C is incomplete.

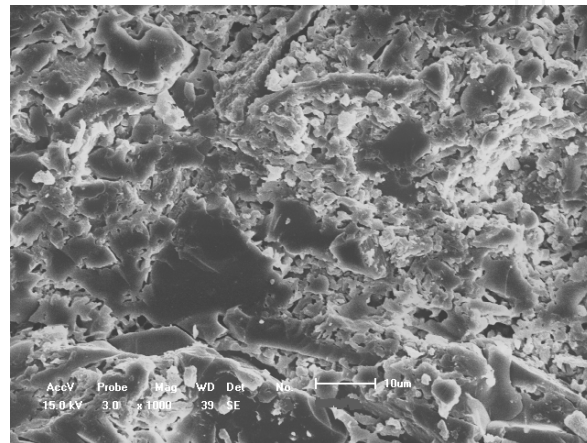


Figure 7. SEM micrograph of the MT1 sample after sintering at 1210 °C.

Fig. 8 shows the fractured surface of the MT1 sample sintered at 1250 °C. It also comprises kaolinite-derivate material (mullite), quartz, and glassy phase. However, the presence of few rounded and isolated pores indicates the consistent development of the liquid phase during sintering. As a consequence, the overall microstructure of the MT1 sintered at 1250 °C is clearly denser.

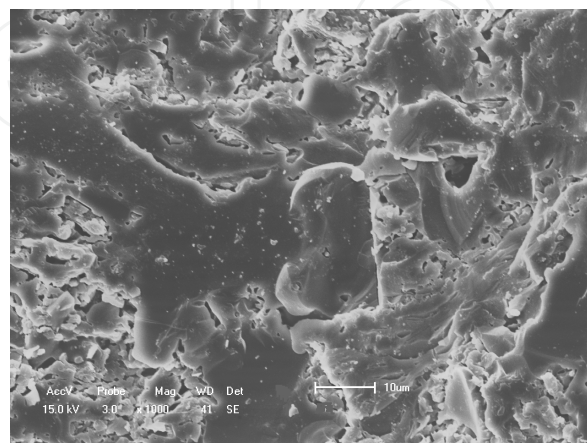


Figure 8. SEM micrograph of the MT1 sample after sintering at 1250 °C.

SEM micrographs of the fractured surfaces of the MT3 sample are presented in Fig. 9a-c. The micrographs show the evolution of the microstructure of the MT3 sample as temperature increases. It may be noted that at 1210 °C (Fig. 9a) and 1230 °C (Fig. 9b), the microstructure is characterized by few nearly spherical isolated pores associated with high degree of vitrification. At 1250 °C (Fig. 9c), however, a more porous fractured surface can be observed. Larger and more irregular pores can be seen. This effect suggests a gas evolution (gas trapped) for higher petroleum waste additions. Thus, the incorporation of petroleum waste into floor tile formulation brought about a relevant variation in the sintered microstructure.

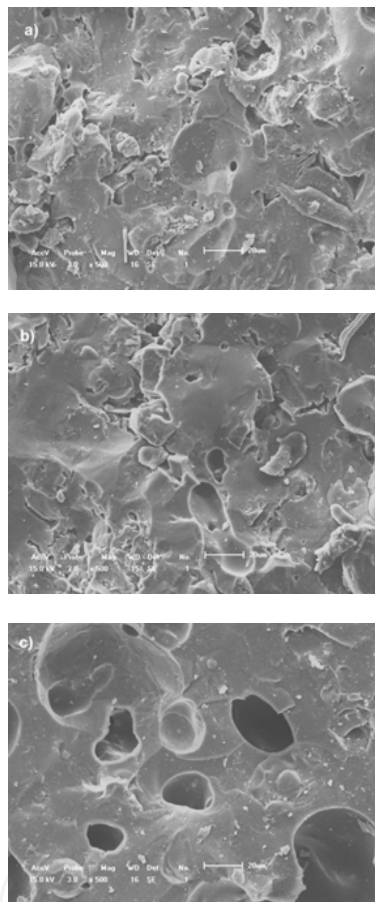


Figure 9. SEM micrographs of the MT3 sample after sintering: a) 1210 °C; b) 1230 °C; and c) 1250 °C.

3.4. Sintering behavior

In the manufacturing process of floor tiles the sintering step is critical. On sintering, the floor tile materials undergo a series of physical and chemical reactions involving dehydroxylation of clay minerals, partial melting of feldspar-quartz eutectic compositions, collapse of the silicate structure to formation of mullite and progressive dissolution of quartz in the liquid phase. These processes play an important role in the sintering behavior of floor tile compositions.

The dilatometric curve of the MT1 sample is shown in Fig. 10. As it can be seen, the sintering behavior of the floor tile formulation is characterized by three main regions. The first region (~ up to 895 °C) is characterized by a negligible shrinkage. The second region within the ~ 900 and 1100 °C temperature range is characterized by a small shrinkage. In this temperature range, the reorganization of the metakaolinite structure and initial formation of the liquid phase occur. In addition, the vitrification of the tile piece is already in progress. The third region (above 1150 °C) is characterized by a considerable shrinkage of the floor tile pieces. It is plausible to consider that an abundant amount of liquid phase was formed, resulting in high densification. This is consistent with the dense microstructure of the MT1 samples sintered at 1250 °C.

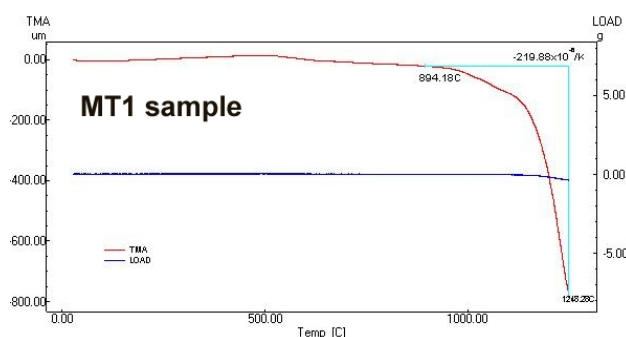


Figure 10. Dilatometric curve of the MT1 sample.

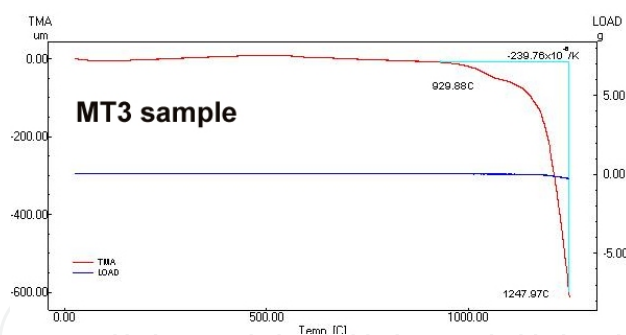


Figure 11. Dilatometric curve of the MT3 sample.

The dilatometric curve of the MT3 sample is shown in Fig. 11. The sintering behavior of the MT3 sample compared with that of the MT1 sample shows small but important differences. It seems that the petroleum waste tends to retard the densification of the tile pieces during sintering. This could be related to the complex composition of the petroleum waste. In fact, the petroleum waste used is composed of several mineral phases and oil (hydrocarbons).

The linear shrinkage of the floor tile pieces is shown in Fig. 12. The linear shrinkage indicates the degree of densification during sintering, and is a physical property very important for dimensional control of the finished tile products.

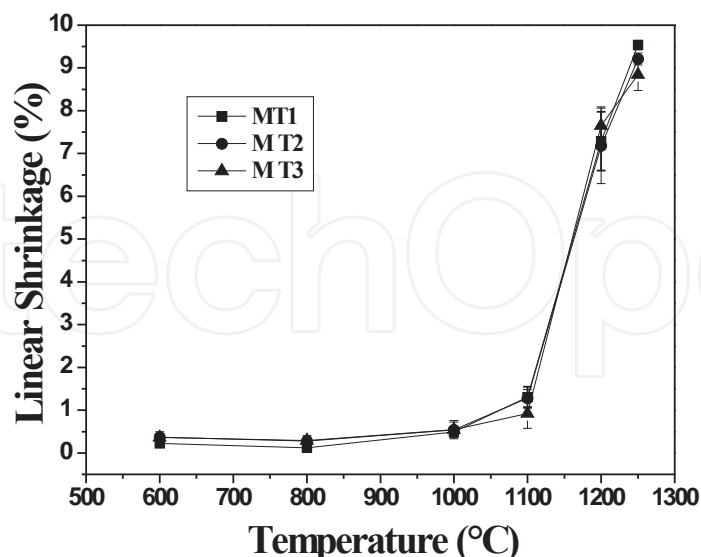


Figure 12. Linear shrinkage of the floor tile samples after sintering.

It is observed that the linear shrinkage presents different behaviors, depending on the sintering temperature range. This is consistent with the dilatometric curves (Figs. 10 and 11). This means that the predominance of distinct sintering mechanisms in their temperature range can occur. In the 600 and 950 °C range, a small linear shrinkage (< 1%) was observed. This low linear shrinkage suggests that the dominant sintering mechanism is surface diffusion [18]. In this temperature range prevails mainly the growth of necks between the mineral particles coupled with significant specific surface area reduction. Moreover, the structural reorganization of matakaolinite and initial melting of quartz-feldspar eutectics are already underway. Between 1000 and 1100 °C, a higher linear shrinkage can be observed. The formation of mullite occurs. The formation of a larger amount of liquid phase also occurs. Above, 1100 °C, however, the linear shrinkage accelerates resulting in high densification of the tile pieces. In this case, the sintering is accompanied by the formation of a significant amount of liquid phase. This liquid phase acts to densify the structure by liquid phase sintering. Viscous flow closing open porosity is the dominant sintering mechanism [19]. It can also be seen in Fig. 12 that the shrinkage tends to be lightly lower for the samples containing petroleum waste. Appearance of the floor tile pieces after sintering is presented in Fig. 13.

The apparent density of the floor tile pieces is shown in Fig. 14. The results show that, in general, the density tends to lightly decrease with petroleum waste addition. Density presents only a small variation up to ~ 1100 °C. This occurred due to the combined inverse effects of sintering and weight loss. As a matter of fact, the green tile pieces when heating up to ~1000 °C underwent weight loss, as shown in Fig. 4. Above 1100 °C, a substantial increase in density is observed. This behavior is in line with the formation of more abundant liquid phase during sintering that fills the open pores. This is consistent with the microstructure (Figs. 8 and 9) and linear shrinkage (Fig. 12).



Figure 13. Appearance of the floor tile pieces after sintering.

The water absorption of the tile pieces is shown in Fig. 15. This property is related to the microstructure, and also determines the open porosity level of the pieces. For sintering temperatures up to ~ 1100 °C, the water absorption remains practically constant. Above 1100 °C, however, a strong decrease in water absorption is measured. This means that the sintering accelerates above 1100 °C and causes densification. The results also showed that the addition of petroleum waste lightly increased the water absorption, except on temperatures above 1100 °C. The variation of the apparent porosity (Fig. 16) is very similar to that observed for the water absorption.

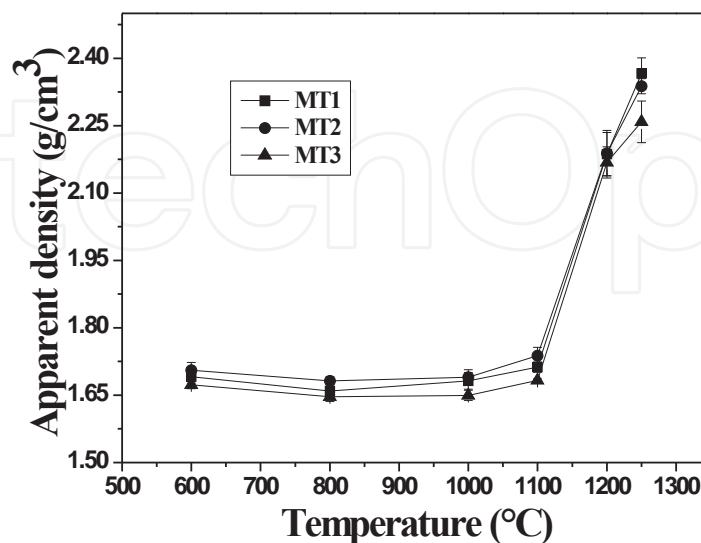


Figure 14. Apparent density of the floor tile samples after sintering.

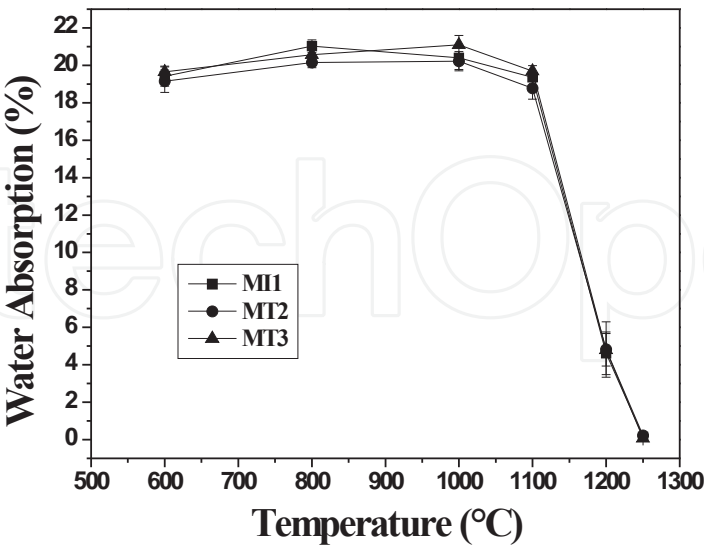


Figure 15. Water absorption of the floor tile samples after sintering.

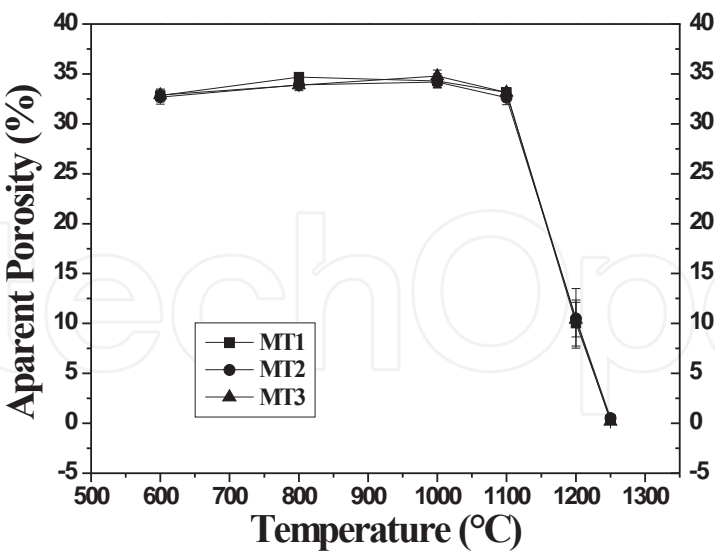


Figure 16. Apparent porosity of the floor tile samples after sintering.

4. Conclusion

In this chapter the sintering behavior of vitrified floor tiles bearing petroleum waste was investigated. It was found that the petroleum waste added influenced the chemical and mineralogical compositions of the floor tile formulations. It was also found that the sintering behavior was influenced by the petroleum waste and sintering temperature. Distinct sintering regions were observed. For the region above 1100 °C, with predominance of the viscous flow sintering mechanism, important changes of the physical properties and sintered microstructure occurred. XRD analysis confirmed the mineralogical changes during sintering. Moreover, it was also observed that the petroleum waste tends retard the densification process of the floor tile pieces. It implies, therefore, that additions of very high petroleum waste amounts in the floor tile formulation should be avoided, because it affects the densification and technical properties of sintered floor tiles.

Acknowledgements

The authors acknowledge the FAPERJ and CNPq for supporting this work.

Author details

A.J. Souza, B.C.A. Pinheiro and J.N.F. Holanda

Northern Fluminense State University - UENF, Laboratory of Advanced Materials – LA-MAV, Group of Ceramic Materials - GMCEr, Campos dos Goytacazes, RJ, Brazil

References

- [1] Curran LM. Waste minimization practices in the petroleum refining industry. *Journal of Hazardous Materials* 1992; 29: 189-97.
- [2] Amaral SP, Domingues GH. Application of oily sludge for manufacturing of ceramic materials. *Proceedings of the 4th Brazilian Congress on Petroleum*, Rio de Janeiro, Brazil, 1990.
- [3] Li X, Lv Y, Ma B, Jian S, Tan H. Influence of sintering temperature on the characteristics of shale brick containing oil well-derived drilling waste. *Environmental Science Pollution Research* 2011; 18: 1617-22.
- [4] Souza GP, Santos RS, Holanda JNF. Recycling of a petroleum waste in ceramic bodies. *Materials Science Forum* 2003; 416-418: 743-7.

- [5] Segadães AM. Use of phase diagrams to guide ceramic production from wastes. *Advances in Applied Ceramics* 2006; 105:46-54.
- [6] Chiang K, Chien K, Hwang S. Study on the characteristics of building bricks produced from reservoir sediment. *Journal of Hazardous Materials* 2008; 159: 499-504.
- [7] Souza AJ, Pinheiro BCA, Holanda JNF. Recycling of gneiss rock waste in the manufacturing of vitrified floor tiles. *Journal of Environmental Management* 2010; 91: 685-89.
- [8] Sengupta P, Saikia N, Borthakur PC. Bricks from petroleum effluent treatment plant sludge: properties and environmental characteristics. *Journal of Environmental Engineering* 2002; 128: 1090-94.
- [9] Acchar W, Rulf BM, Segadães AM. Effect of the incorporation of a spent catalyst reject from the petroleum industry in clay products. *Applied Clay Science* 2009; 42: 657-60.
- [10] El-Mahllawy MS, Osman TA. Influence of oil well drilling waste on the engineering characteristics of clay bricks. *Journal of American Science* 2010; 6(7): 48-54.
- [11] Souza AJ, Pinheiro BCA, Holanda JNF. Valorization of solid petroleum waste as a potential raw material for clay-based ceramics. *Waste and Biomass Valorization* 2011; 2:381-88.
- [12] Manfredini T, Pellacani GC, Romagnali M. Porcelain stoneware tiles. *American Ceramic Society Bulletin* 1995 ; 74 : 76-79.
- [13] ASTM, ASTM C373 – Test method for water absorption, bulk density, apparent porosity, and apparent specific gravity of fired whiteware products, 1994.
- [14] Brindley GW, Nakahira N. The kaolinite-mullite reactions:II, metakaolin. *Journal of the American Ceramic Society* 1959; 42: 314-18.
- [15] Brindley GW, Nakahira N. The kaolinite-mullite reactions:III, high temperature phases. *Journal of the American Ceramic Society* 1959; 42: 319-23.
- [16] Barba A, Beltrán V, Fileu C, García J, Ginés F, Sanchez E, Sanz V. *Materias Primas Para la Fabricación de Soportes de Baldosas Cerámicas*. 2nd Ed. Castellón: ITC; 2002.
- [17] Sousa SJG, Holanda JNF. Thermal transformations of red wall tiles. *Journal of Thermal Analysis and Calorimetry* 2007; 87: 423-8.
- [18] Kingery WD, Berg M. Study of the initial stages of sintering solids by viscous flow, evaporation-condensation, and self-diffusion. *Journal of Applied Physics* 1955; 26 (10) 1205-12.
- [19] Kingery WD, Bowen HK, Uhlmann DR. *Introduction to Ceramics*. 2nd ed. New York: Wiley; 1976.